Subphthalocyanine-Stoppered [2]Rotaxanes: Synthesis and Size/Energy Threshold of Slippage

Yuto Kage,[†] Soji Shimizu*[,†,‡] Gabriele Kociok-Köhn,[§] Hiroyuki Furuta,[†,‡] and G. Dan Pantoş*[,§]

[†]Department of Chemistry and Biochemistry, Graduate School of Engineering, Kyushu University, Fukuoka 819-0395, Japan

[‡]Center for Molecular Systems (CMS), Kyushu University, Fukuoka 819-0395, Japan

[§]Department of Chemistry, University of Bath, Bath BA2 7AY, U.K.

Supporting Information Placeholder

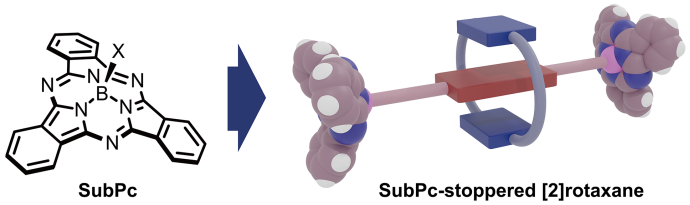

ABSTRACT: Subphthalocyanine (SubPc)-stoppered [2]rotaxanes were synthesized for the first time. The rotaxane bearing unsubstituted SubPc as a stopper exhibited equilibrium of slipping-on and slipping-off, whereas a perfluorinated SubPc stopper completely blocked slippage of the ring due to its slightly larger size. Kinetics studies revealed the Gibbs free energy of activation for the slipping-on and slipping-off processes. The optical properties of the rotaxanes including photo-induced electron transfer (PET) were also revealed.

Rotaxanes are a class of mechanically interlocked molecules (MIMs) that have been intensively researched due to their potential use in molecular machines.[1–3] The function of molecular machines can be attained by controlling the mobility of rotaxanes using external stimuli. In this context, functional dye molecules are promising building blocks due to their optical and redox properties and interactions with π-conjugated molecules. For example, porphyrin-based rotaxanes have been intensively studied to develop charge-transfer systems,[4–8] high-order rotaxane assemblies,[9–12] catalysis[13,14] and so on.[15] Other dye molecules such as phthalocyanine,[16,17] boron-dipyrromethene,[18] diketopyrrolopyrrole,[19] squarene,[20] rhodamine,[21] and perylene diimide[22] were also investigated as building blocks of rotaxanes. However, the number of dye molecules available for rotaxane syntheses is still limited, and broadening their variety is important.

Subphthalocyanine (SubPc) is a ring-contracted homologue of phthalocyanine.[23] Its intriguing electronic and optical properties have allowed chemists to investigate several applications such as organic photovoltaics[24–27] and organic light emitting diodes.[24,28] SubPc has a bowl-shaped structure with an axial ligand on the central boron atom. Despite this unique structure in terms of supramolecular chemistry, only a few examples of SubPc-based supramolecular architectures have been reported so far. Torres and Claessens reported cage structures of SubPc and self-assembly of SubPcs with C_{60}.[29] Homochiral supramolecular polymers of SubPcs and their ferroelectric properties were reported by González-Rodríguez *et al.*[30,31] The group of Watarai reported supramolecular complex of SubPc-cyclodextrin assemblies.[32] A similar assembly was also reported by Ng *et al.*[33] These works indicate the advantage of the bowl-shaped structure bearing an axial ligand for creating MIMs, because of unique interactions such as concave-convex π-π interactions. However, as far as we know, a SubPc-based MIM has not been reported yet.

Here, we describe the first synthesis of SubPc-stoppered [2]rotaxanes using donor-acceptor interaction between naphthalene diimide (NDI) and dialkoxy-substituted naphthalene (DN). Slippage behaviours of the ring unit depending on the size of SubPc stoppers were also investigated.

Starting from unsubstituted SubPc (**1-H**) and perfluorinated SubPc (**1-F**), the target [2]rotaxanes were synthesized (Scheme 1). The axial ligand of the central boron was activated by replacing Cl with OTf using AgOTf.[34] *N,N'*-di(5-hydroxypentyl)-1,4,5,8-naphthalene diimide[35] was, then, reacted under microwave irradiation to afford doubly-capped axles, **3-H** (9%) and **3-F** (3%), and singly-capped axles, **3'-H** (40%) and **3'-F** (12%), respectively. The use of excess amount of NDI caused formation of **3'-H** and **3'-F** as main products. Fortunately, single crystals of **3-H** and **3'-H** suitable for X-ray diffraction analysis were obtained (Figure 1). In the crystal structure of **3-H**, intermolecular π-π

interactions between neighboring SubPc and NDI and those between SubPcs were observed (Figures S18 and S19). In the case of **3'-H**, intermolecular π-π interactions between neighboring NDIs and SubPcs were also observed in addition to the similar interactions observed for **3-H** (Figures S20

Scheme 1. Synthesis of SubPc-stoppered [2]rotaxanes.

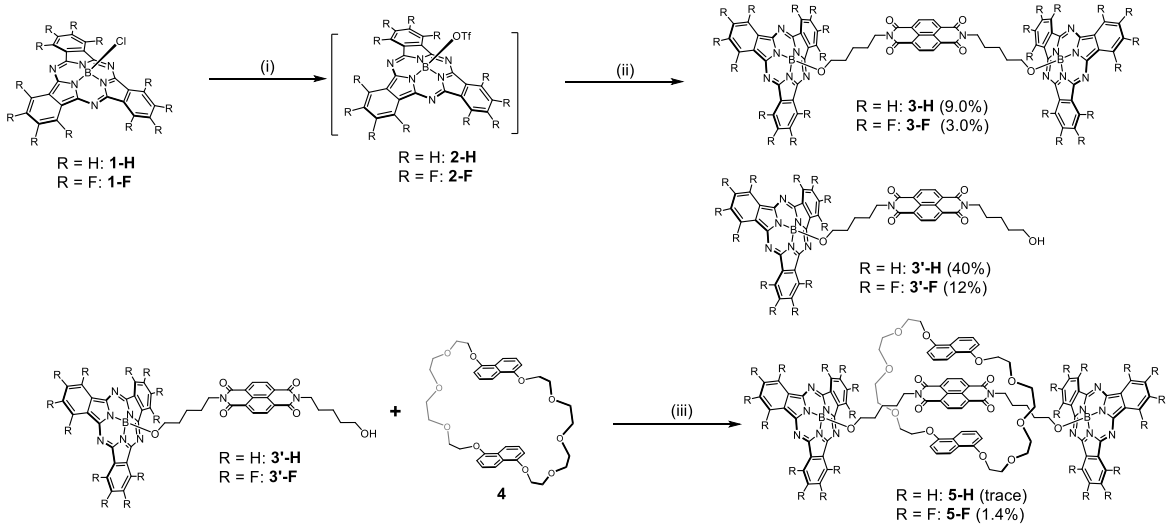

Reagents and conditions: (i) AgOTf, toluene, r.t. (R = H) or reflux (R = F), N_2; (ii) *N,N'*-di(5-hydroxypentyl)-1,4,5,8-naphthalene diimide, NEt_3, toluene, μW 155 °C, N_2; (iii) **2-H** (R = H) or **2-F** (R = F), NEt_3, toluene, 40 °C, N_2.

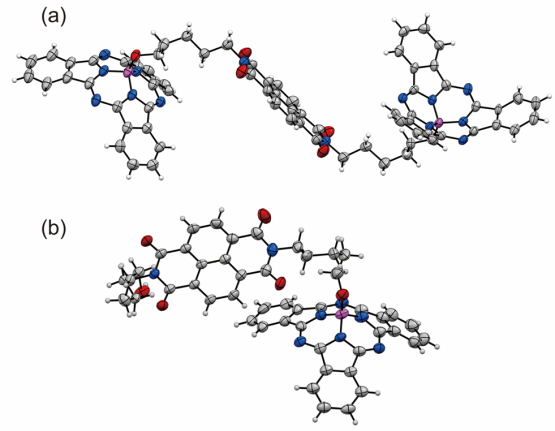

Figure 1. X-ray crystal structures of (a) **3-H** and (b) **3'-H**. The thermal ellipsoids were scaled at 50%.

and S21).

To convert **3'-H** and **3'-F** to the corresponding [2]rotaxanes, **3'-H** and **3'-F** were at first mixed with the DN ring (**4**). This mixture was reacted with axially activated SubPcs (**2-H** and **2-F**) for a few days to give the target rotaxane molecules, **5-H** (trace) and **5-F** (1.4%). All compounds were fully characterized by NMR spectroscopy (Figures 2 and S1–S16) and high-resolution mass spectrometry (Figures S22–S27).

In the ^{1}H NMR spectra, the signals from the NDI in the axle and those from the DNs in the ring of **5-H** and **5-F** shifted upfield compared with **3-H**, **3-F** and **4**. Similar upfield shifts were also reported for other rotaxanes,[36] indicating the axles were successfully threaded through the DN rings. The threading was further confirmed by ROESY, which showed a NOE contact between the NDI proton and the ethylene glycol chain of the DN ring (Figure S16). However, in the ^{1}H NMR spectrum of **5-H**, a weak, but distinct signal of the NDI proton of **3-H** was observed at 8.61 ppm. Upon recrystallization of **5-H** from a chloroform/hexane solution, we noticed further intensification of this NDI signal. Meanwhile, **5-H** was generated after storing **3-H** and **4** in chloroform at room temperature for several hours.

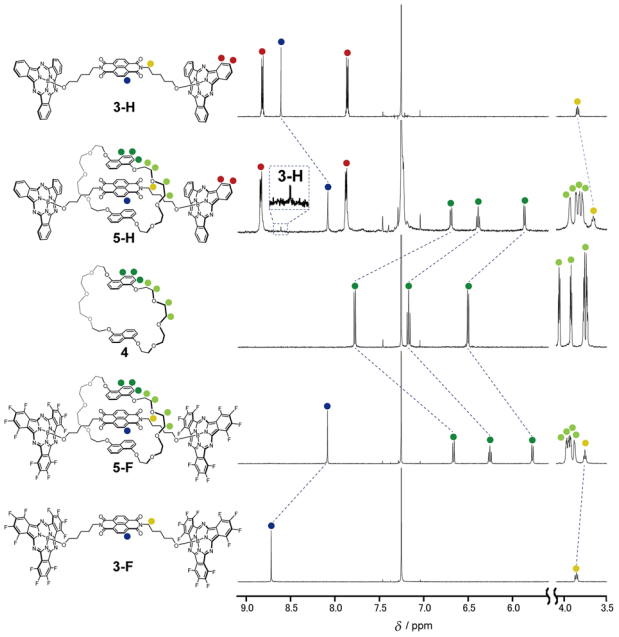

Figure 2. ^{1}H NMR spectra of **3-H**, **5-H**, **4**, **3-F**, and **5-F** in $CDCl_3$.

These results clearly indicate slipping-on and -off behavior of
the DN ring. In contrast, **5-F** did not show such a behavior. Pure **5-F** was isolated by recrystallization, whereas a mixture of **3-F** and **4** did not provide **5-F** either at room temperature or at elevated temperatures (Figure S28).

The different slippage behaviors can be ascribed to slight difference in size between unsubstituted SubPc and perfluorinated SubPc. In the crystal structures of SubPcs with phenoxy axial ligands,[28,37] the distances from the central boron atom to the edge of the peripheral hydrogen atom and fluorine atom in van der Waals model are 8.13 Å for unsubstituted SubPc and 8.75 Å for perfluorinated SubPc, respectively (Figure S29). The stopper size threshold of slippage can, therefore, fall between the size of unsubstituted SubPc and that of perfluorinated SubPc. The radius of tris(4-(*t*-butyl)phenyl)methyl stopper, which can block both slipping-on and -off of **4**, was reported to be 8.53 Å.[36] The estimated threshold is reasonable although the molecular shapes of SubPc and tris(4-(*t*-butyl)phenyl)methyl stopper are different (Figure S29). This indicates that a small difference in size between unsubstituted and perfluorinated SubPcs critically affected the slippage behavior.

To give in-depth insight into the dynamic slippage behavior of **5-H**, kinetics studies were performed by ^{1}H NMR spectroscopy. The rate constant can be estimated from Equations (1)–(4).[38]

$$\mathbf{A} + \mathbf{Ring} \underset{k_{off}}{\overset{k_{on}}{\rightleftarrows}} \mathbf{R} \quad (1)$$

$$\boldsymbol{X} \ln \boldsymbol{Y} = \boldsymbol{k_{on} t} \quad (2)$$

$$\boldsymbol{X} = \frac{\boldsymbol{c_e}}{\boldsymbol{c_0^2 - c_e^2}} \quad (3)$$

$$\boldsymbol{Y} = \frac{\boldsymbol{c_e}(\boldsymbol{c_0^2 - c_e}[\boldsymbol{R}])}{\boldsymbol{c_0^2}(\boldsymbol{c_e} - [\boldsymbol{R}])} \quad (4)$$

where **A**, **Ring**, and **R** refer to axle, ring, and rotaxane, respectively. c_0, c_e, and [***R***] are the concentrations of axle at the initial state, rotaxane at the equilibrium state, and rotaxane at time *t*. k_{on} and k_{off} are rate constants for the slipping-on and slipping-off of the ring. Among these variables, c_e and [***R***] can be experimentally determined by ^{1}H NMR spectroscopy, and c_0 is known. The experiments were performed using a solution containing a 1:1 mixture of **3-H** and **4** (3.6 mM for both) in $CDCl_3$ at three different temperatures (298, 308, and 318 K). After mixing **3-H** and **4** in $CDCl_3$, ^{1}H NMR spectra were recorded every 10 or 30 min (Figure 3a). The integral ratio of the signals of **3-H** and **5-H** gradually changed as time proceeded. By plotting the concentration changes of **5-H** against time, k_{on} was estimated (Tables 1 and S3 and Figures S30–S35). Then, k_{off} and the association constant, K_a, were determined. K_a decreased upon increasing the temperature, which is consistent with the entropically unfavorable slipping-on process. Eyring plot analysis was also performed for both slipping-on and slipping-off processes, and the activation Gibbs free energy for slipping-on at 298 K, $\Delta G^{\ddagger}_{on,298\,K}$, was determined to be 19.5 kcal mol^{-1}, whereas that for slipping-off, $\Delta G^{\ddagger}_{off,298\,K}$, was 22.1 kcal mol^{-1} (Figures 3b, c and Table 1). The Gibbs free energy of the reaction, $\Delta G^{\circ}_{on,298\,K}$, was estimated to be −2.6 kcal mol^{-1} (Table 2 and Figure 4). These small $\Delta G^{\ddagger}_{on,298\,K}$ and $\Delta G^{\circ}_{on,298\,K}$ values, which corresponds to the small $\Delta G^{\ddagger}_{off,298\,K}$, allowed **5-H** to dissociate into **3-H** and **4** at room temperature.

$\Delta G^{\ddagger}_{on,298\,K}$ and $\Delta G^{\ddagger}_{off,298\,K}$ are kinetic terms relating to the size effects of the SubPc stopper. Considering that the perfluorinated SubPc is larger than the size threshold of slippage, partial fluorination of **1-H** enables controlling the $\Delta G^{\ddagger}_{on,298\,K}$ and $\Delta G^{\ddagger}_{off,298\,K}$ values. The $\Delta G^{\circ}_{on,298\,K}$ value is a thermodynamic term which is decomposed into an enthalpy term, ΔH°_{on}, of −10.4 kcal mol^{-1} and an entropy term, ΔS°_{on}, of −0.0259 kcal K^{-1}mol^{-1}. Compared with other slippage systems where slipping-on is allowed and slipping-off is prohibited,[38] ΔS°_{on} of **3-H** and **4** is larger, while ΔH°_{on} is a similar value. The dissociation of **5-H** can, therefore, be ascribed to the negative ΔS°_{on}.

The slippage synthesis, which was proposed by Stoddart *et al.*, is known as a high-yield synthesis of rotaxane molecules.[38] Despite its great potential, only a few systems have been established because the size/energy tuning is critical. The partial

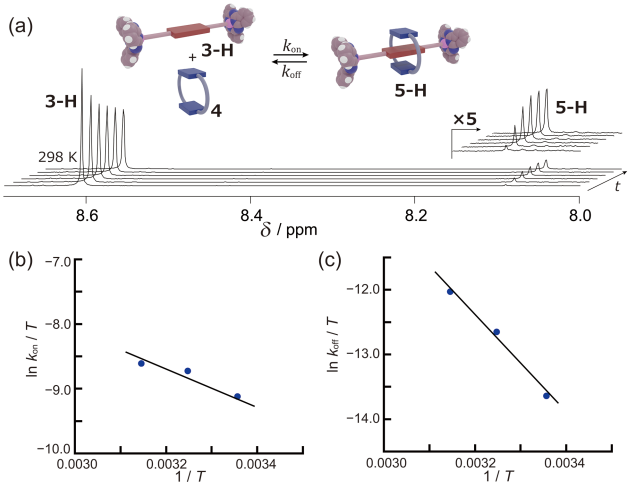

Figure 3. (a) Spectral changes of ^{1}H NMR signals after mixing **3-H** and **4** in $CDCl_3$ at 298 K (inset: Schematic image of the slippage behavior of **5-H**). Eyring plots of (b) slipping-on and (c) slipping-off processes in $CDCl_3$.

Table 1. Kinetic parameters of the slippage of **5-H**.

T / K	k_{on} / M^{-1}s^{-1}	k_{off} / s^{-1}	K_a / M^{-1}
298	2.79 × 10^{-3}	3.04 × 10^{-5}	91.5
308	5.80 × 10^{-3}	1.14 × 10^{-4}	50.7
318	8.35 × 10^{-3}	2.74 × 10^{-4}	30.5

Table 2. Thermodynamic parameters of the slippage of **5-H**.

$\Delta H^{\ddagger}_{on}$ / kcal mol^{-1}	$\Delta S^{\ddagger}_{on}$ / kcal K^{-1}mol^{-1}	$\Delta G^{\ddagger}_{on,298\,K}$ / kcal mol^{-1}
4.8	−0.0491	19.5
$\Delta H^{\ddagger}_{off}$ / kcal mol^{-1}	$\Delta S^{\ddagger}_{off}$ / kcal K^{-1}mol^{-1}	$\Delta G^{\ddagger}_{off,298\,K}$ / kcal mol^{-1}
15.2	−0.0232	22.1
ΔH°_{on} / kcal mol^{-1}	ΔS°_{on} / kcal K^{-1}mol^{-1}	$\Delta G^{\circ}_{on,298\,K}$ / kcal mol^{-1}
−10.4	−0.0259	−2.6

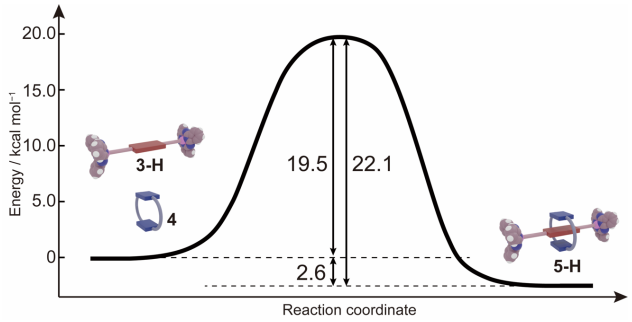

Figure 4. Energy diagram for the formation of **5-H** by slippage.

fluorination of the SubPc stopper might achieve the critical size. In energetic terms, solvents at the opposite ends of the polarity scale decrease the ΔS°_{on} value because the donor-acceptor interactions between NDI and DN are enhanced with increasing solvent polarity,[39] or by decreasing it to the low polarity of aliphatic solvent.[40] The slippage synthesis of SubPc-stoppered rotaxanes can also be realized by a careful choice of solvent.

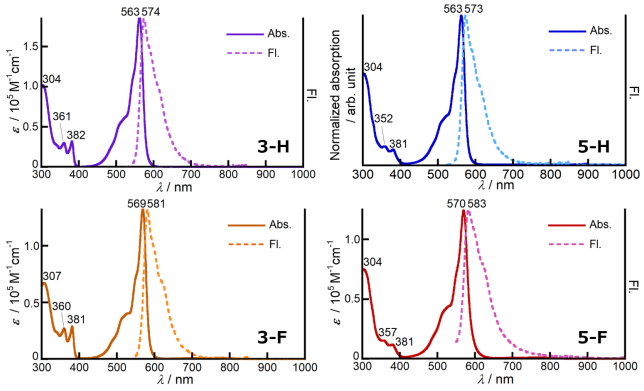

Figure 5. UV/Vis absorption (solid line) and fluorescence (dashed line) spectra of **3-H**, **3-F**, **5-H**, and **5-F** in $CHCl_3$.

In chloroform, **3-H** and **5-H** both showed absorption at 563 nm and fluorescence at 574 and 573 nm with fluorescence quantum yields of 0.016 and 0.014, respectively (Figure 5). The sharp absorption and fluorescence bands, which were similar to those of regular SubPcs indicated the absence of effective electronic interactions between the SubPc stoppers and the NDI axle or the DN ring at the ground state. The lower fluorescence quantum yields compared to that of unsubstituted SubPc (ca. 0.30) were ascribed to photo-induced electron transfer (PET) from the SubPc stoppers to the NDI axle, as with the case reported by Fukuzumi *et al.*[41] **3-F** and **5-F** also showed sharp absorption at 569 and 570 nm, and fluorescence at 581 and 583 nm, respectively. Interestingly, **3-F** was highly fluorescent, and its fluorescence quantum yield was 0.15. This may be explained in terms of the stabilized LUMO level by the peripheral fluorine atoms, which might prevent the PET process. In the case of **5-F**, the fluorescence quantum yield dropped to 0.013, indicating a PET from the DN ring to the SubPc stoppers. When all the absorption spectra were carefully compared, **5-F** showed slight broadening of the absorption band (Figure S36). This suggests that the DN ring of **5-F** is in the vicinity of the perfluorinated SubPc stopper, which is also supported by the upfield shifts of the protons in the DN ring of **5-F** compared with those of **5-H** in the ^{1}H NMR spectra (Figure S17).

In conclusion, we achieved the first synthesis of SubPc-stoppered [2]rotaxanes and revealed the slippage behavior as well as the two different PET processes. The Gibbs free energies of activation for the slipping-on and slipping-off were determined to be 19.5 and 22.1 kcal mol^{-1}. This work adds SubPc to the molecular toolbox for designing rotaxanes with the slippage energy/size threshold, which gives important directions of molecular design toward the slippage synthesis.[38] The tunable nature of the SubPc stopper as electron donor or acceptor in PET also enables various molecular design of rotaxane-based charge-transfer systems, indicating high potential of SubPc in terms of not only a useful stopper for rotaxane synthesis but also its functions.

ASSOCIATED CONTENT

Supporting Information

The Supporting Information is available free of charge on the ACS Publications website.

Experimental procedures, ^{1}H, ^{13}C, and ^{19}F NMR spectra, ^{1}H-^{1}H COSY and ROESY spectra, crystallographic data, HRMS spectra, size comparison of the stoppers, kinetics studies, and absorption spectra (PDF).

Accession Codes

CCDC 1953453 and 1953454 contain the supplementary crystallographic data for this paper. These data can be obtained free of charge via www.ccdc.cam.ac.uk/data_request/cif, or by emailing data_request@ccdc.cam.ac.uk, or by contacting The Cambridge Crystallographic Data Centre, 12 Union Road, Cambridge CB2 1EZ, UK; fax: +44 1223 336033.

AUTHOR INFORMATION

Corresponding Author

* E-mail: ssoji@cstf.kyushu-u.ac.jp.
* E-mail: gp304@bath.ac.uk

ORCID

Soji Shimizu: 0000-0002-2184-7468
Hiroyuki Furuta: 0000-0002-3881-8807
G. Dan Pantoş: 0000-0003-2200-550X

Notes

The authors declare no competing financial interest.

ACKNOWLEDGMENT

This work was funded by the GW4 consortium (GW4-AF5-002), the University of Bath, and Grants-in-Aid for JSPS Fellows (JSPS KAKENHI Grant Number JP19J12257). YK thanks the Kyushu University Leading Program for "Molecular System for Devices" from MEXT Japan. YK is also grateful to Mr. Tiberiu M. Gianga and Ms. Dora M. Rasădean at the University of Bath for their great help and advice about molecular design and characterization.

REFERENCES

(1) Bruns, C. J.; Stoddart, F. J. Rotaxane-Based Molecular Muscles. *Acc. Chem. Res.* **2014**, *47*, 2186–2199.
(2) Yang, W.; Li, Y.; Liu, H.; Chi, L.; Li, Y. Design and Assembly of Rotaxane-Based Molecular Switches and Machines. *Small*, **2012**, *8*, 504–516.

(3) Xue, M.; Yang, Y.; Chi, X.; Yan, X.; Huang, F. Development of Pseudorotaxanes and Rotaxanes: From Synthesis to Stimuli-Responsive Motions to Applications. *Chem. Rev.* **2015**, *115*, 7398–7501.
(4) (a) Chambron, J.; Harriman, A.; Heitz, V.; Sauvage, J.-P. Ultrafast Photoinduced Electron Transfer between Porphyrinic Subunits within a Bis(Porphyrin)-Stoppered Rotaxane. *J. Am. Chem. Soc.* **1993**, *115*, 6109–6114. (b) Linke, M.; Chambron, J.-C.; Heitz, V.; Sauvage, J.-P.; Encinas, S.; Barigelletti, F.; Flamigni, L. Multiporphyrinic Rotaxanes: Control of Intramolecular Electron Transfer Rate by Steering the Mutual Arrangement of the Chromophores. *J. Am. Chem. Soc.* **2000**, *122*, 11834–11844. (c) Andersson, M.; Linke, M.; Chambron, J.-C.; Davidsson, J.; Heitz, V.; Hammarström, L.; Sauvage, J.-P. Long-Range Electron Transfer in Porphyrin-Containing [2]-Rotaxanes: Tuning the Rate by Metal Cation Coordination. *J. Am. Chem. Soc.* **2002**, *124*, 4347–4362.
(5) (a) Watanabe, N.; Kihara, N.; Furusho, Y.; Takata, T.; Araki, Y.; Ito, O. Photoinduced Intrarotaxane Electron Transfer between Zinc Porphyrin and [60]Fullerene in Benzonitrile. *Angew. Chem. Int. Ed.* **2003**, *42*, 681–683. (b) Sandanayaka, A. S.; Sasabe, H.; Araki, Y.; Kihara, N.; Furusho, Y.; Takata, T.; Ito, O. Axle Length Effect on Photoinduced Electron Transfer in Triad Rotaxane with Porphyrin, [60]Fullerene, and Triphenylamine. *J. Phys. Chem. A* **2010**, *114*, 5242–5250.
(6) Li, K.; Bracher, P. J.; Guldi, D. M.; Herranz, Á. M.; Echegoyen, L.; Schuster, [60]Fullerene-Stoppered Porphyrinorotaxanes: Pronounced Elongation of Charge-Separated-State Lifetimes. D. I. *J. Am. Chem. Soc.* **2004**, *126*, 9156–9157.
(7) Delavaux-Nicot, B.; Aziza, H. B.; Nierengarten, I.; Trinh, T. M. N.; Meichsner, E.; Chessé, M.; Holler, M.; Abidi, R.; Maisonhaute, E.; Nierengarten, J.-F. A Rotaxane Scaffold for the Construction of Multiporphyrinic Light-Harvesting Devices. *Chem. –Eur. J.* **2018**, *24*, 133–140.
(8) Wolf, M.; Ogawa, A.; Bechtold, M.; Vonesch, M.; Wytko, J. A.; Oohora, K.; Campidelli, S.; Hayashi, T.; Guldi, D. M.; Weiss, J. Light Triggers Molecular Shuttling in Rotaxanes: Control over Proximity and Charge Recombination. *Chem. Sci.* **2019**, *10*, 3846–3853.
(9) (a) Yamada, Y.; Okamoto, M.; Furukawa, K.; Kato, T.; Tanaka, K. Switchable Intermolecular Communication in a Four-Fold Rotaxane. *Angew. Chem. Int. Ed.* **2012**, *51*, 709–713. (b) Yamada, Y.; Mihara, N.; Shibano, S.; Sugimoto, K.; Tanaka, K. Triply Stacked Heterogeneous Array of Porphyrins and Phthalocyanine through Stepwise Formation of a Fourfold Rotaxane and an Ionic Complex. *J. Am. Chem. Soc.* **2013**, *135*, 11505–11508.
(10) Zhang, H.; Liu, Q.; Li, J.; Qu, D.-H. A Novel Star-Shaped Zinc Porphyrin Cored [5]Rotaxane. *Org. Lett.* **2013**, *15*, 338–341.
(11) Ngo, T.; Labuta, J.; Lim, G.; Webre, W.; D'Souza, F.; Karr, P.; Lewis, J.; Hill, J.; Ariga, K.; Goldup, S. M. Porphyrinoid Rotaxanes: Building a Mechanical Picket Fence. *Chem. Sci.* **2017**, *8*, 6679–6685.
(12) Kohn, D. R.; Movsisyan, L. D.; Thompson, A. L.; Anderson, H. L. Porphyrin-Polyyne [3]- and [5]Rotaxanes. *Org. Lett.* **2017**, *19*, 348–351.
(13) Thordarson, P.; Bijsterveld, E. J.; Rowan, A. E.; Nolte, R. J. Epoxidation of Polybutadiene by a Topologically Linked Catalyst. *Nature*, **2003**, *424*, 915–918.
(14) Mihara, N.; Yamada, Y.; Takaya, H.; Kitagawa, Y.; Igawa, K.; Tomooka, K.; Fujii, H.; Tanaka, K. Site-Selective Supramolecular Complexation Activates Catalytic Ethane Oxidation by a Nitrido-Bridged Iron Porphyrinoid Dimer. *Chem. –Eur. J.* **2019**, *25*, 3369–3375.
(15) Ma, X.; Zhang, J.; Cao, J.; Yao, X.; Cao, T.; Gong, Y.; Zhao, C.; Tian, H. A Room Temperature Phosphorescence Encoding [2]Rotaxane Molecular Shuttle. *Chem. Sci.* **2016**, *7*, 4582–4588.
(16) Kirner, S. V.; Henkel, C.; Guldi, D. M.; Megiatto Jr, J. D.; Schuster, D. I. Multistep Energy and Electron Transfer Processes in Novel Rotaxane Donor–Acceptor Hybrids Generating Microsecond-Lived Charge Separated States. *Chem. Sci.* **2015**, *6*, 7293–7304.
(17) Yamada, Y.; Kato, T.; Tanaka, K. Assembly of Multi-Phthalocyanines on a Porphyrin Template by Fourfold Rotaxane Formation. *Chem. –Eur. J.* **2016**, *22*, 12371–12380.
(18) Sun, N.; Xiao, X.; Li, W.; Jiang, J. Multistimuli Sensitive Behavior of Novel Bodipy-Involved Pillar[5]Arene-Based Fluorescent [2]Rotaxane and Its Supramolecular Gel. *Adv. Sci.* **2015**, *2*, 1500082–1500090.
(19) (a) Raju, M. V.; Lin, H.-C. A Novel Diketopyrrolopyrrole (DPP)-Based [2]Rotaxane for Highly Selective Optical Sensing of Fluoride. *Org. Lett.* **2013**, *15*, 1274–1277. (b) Raju, M. V.; Raghunath, P.; Lin, M.-C.; Lin, H.-C. An Acid-Base Controllable Hierarchical Nanostructure from a NIR-Absorbing Conjugated Polyrotaxane-Based Optical Molecular Switch. *Macromolecules*, **2013**, *46*, 6731–6743.
(20) (a) Arunkumar, E.; Forbes, C. C.; Noll, B. C.; Smith, B. D. Squaraine-Derived Rotaxanes: Sterically Protected Fluorescent Near-IR Dyes. *J. Am. Chem. Soc.* **2005**, *127*, 3288–3289. (b) Johnson, J. R.; Fu, N.; Arunkumar, E.; Leevy, M. W.; Gammon, S. T.; Piwnica-Worms, D.; Smith, B. D. Squaraine Rotaxanes: Superior Substitutes for Cy-5 in Molecular Probes for Near-Infrared Fluorescence Cell Imaging. *Angew. Chem. Int. Ed.* **2007**, *46*, 5528–5531. (c) Gassensmith, J. J.; Matthys, S.; Lee, J.; Wojcik, A.; Kamat, P. V.; Smith, B. D. Squaraine Rotaxane as a Reversible Optical Chloride Sensor. *Chem. –Eur. J.* **2010**, *16*, 2916–2921. (d) Peck, E. M.; Collins, C. G.; Smith, B. D. Thiosquaraine Rotaxanes: Synthesis, Dynamic Structure, and Oxygen Photosensitization. *Org. Lett.* **2013**, *15*, 2762–2765. (e) Collins, C. G.; Peck, E. M.; Kramer, P. J.; Smith, B. D. Squaraine Rotaxane Shuttle as a Ratiometric Deep-Red Optical Chloride Sensor. *Chem. Sci.* **2013**, *4*, 2557–2563.
(21) Shi, J.; Xu, Y.; Wang, X.; Zhang, L.; Zhu, J.; Pang, T.; Bao, X. Synthesis and Evaluation of a Novel Rhodamine B Pyrene [2]Rotaxane as an Intracellular Delivery Agent for Doxorubicin. *Org. Biomol. Chem.* **2015**, *13*, 7517–7529.
(22) Barendt, T.; Ferreira, L.; Marques, I.; Felix, V.; Beer, P. D. Anion- and Solvent-Induced Rotary Dynamics and Sensing in a Perylene Diimide [3]Catenane. *J. Am. Chem. Soc.* **2017**, *139*, 9026–9037.
(23) Claessens, C. G.; González-Rodríguez, D.; Rodríguez-Morgade, S. M.; Medina, A.; Torres, T. Subphthalocyanines, Subporphyrazines, and Subporphyrins: Singular Nonplanar Aromatic Systems. *Chem. Rev.* **2014**, *114*, 2192–2277.
(24) Morse, G. E.; Bender, T. P. Boron Subphthalocyanines as Organic Electronic Materials. *ACS Appl. Mater. Inter.* **2012**, *4*, 5055–5068.
(25) (a) Cnops, K.; Zango, G.; Genoe, J.; Heremans, P.; Martinez-Diaz, V. M.; Torres, T.; Cheyns, D. Energy Level Tuning of Non-Fullerene Acceptors in Organic Solar Cells. *J. Am. Chem. Soc.* **2015**, *137*, 8991–8997. (b) Duan, C.; Zango, G.; Iglesias, M.; Colberts, F. J.; Wienk, M. M.; Martínez-Díaz, V. M.; Janssen, R. A.; Torres, T. The Role of the Axial Substituent in Subphthalocyanine Acceptors for Bulk-Heterojunction Solar Cells. *Angew. Chem. Int. Ed.* **2017**, *56*, 148–152.
(26) Sampson, K. L.; Josey, D. S.; Li, Y.; Virdo, J. D.; Lu, Z.-H.; Bender, T. P. Ability To Fine-Tune the Electronic Properties and Open-Circuit Voltage of Phenoxy-Boron Subphthalocyanines through Meta-Fluorination of the Axial Substituent. *J. Phys. Chem. C* **2018**, *122*, 1091–1102.
(27) Huang, X.; Hu, M.; Zhao, X.; Li, C.; Yuan, Z.; Liu, X.; Cai, C.; Zhang, Y.; Hu, Y.; Chen, Y. Subphthalocyanine Triimides: Solution Processable Bowl-Shaped Acceptors for Bulk Heterojunction Solar Cells. *Org. Lett.* **2019**, *21*, 3382–3386.
(28) Morse, G. E.; Helander, M. G.; Maka, J. F.; Lu, Z.-H.; Bender, T. P. Fluorinated Phenoxy Boron Subphthalocyanines in Organic Light-Emitting Diodes. *ACS Appl. Mater. Inter.* **2010**, *2*, 1934–1944.
(29) (a) Claessens, C. G.; Torres, T. Chiral Self-Discrimination in a M_3L_2 Subphthalocyanine Cage. *J. Am. Chem. Soc.* **2002**, *124*, 14522–14523. (b) Claessens, C. G.; Torres, T. Inclusion of C_{60} Fullerene in a M_3L_2 Subphthalocyanine Cage. *Chem. Commun.* **2004**, 1298–1299. (c) Sánchez-Molina, I.; Claessens, C. G.; Grimm, B.; Guldi, D. M.; Torres, T. Trapping fullerenes with jellyfish-like

subphthalocyanines. *Chem. Sci.* **2013**, *4*, 1338–1344. (d) Sánchez-Molina, I.; Grimm, B.; Calderon, R. M. K.; Claessens, C. G.; Guldi, D. M.; Torres, T. Self-Assembly, Host–Guest Chemistry, and Photophysical Properties of Subphthalocyanine-Based Metallosupramolecular Capsules. *J. Am. Chem. Soc.* **2013**, *135*, 10503–10511. (e) Sánchez-Molina, I.; Ince, M.; Bottari, G.; Claessens, C. G.; Martinez-Diaz, M. V.; Torres, T. Encapsulation of phthalocyanine-C_{60} fullerene conjugates into metallosupramolecular subphthalocyanine capsules: a turn of the screw. *Turk. J. Chem.* **2014**, 38, 1006–1012.

(30) Guilleme, J.; Mayoral, M. J.; Calbo, J.; Aragó, J.; Viruela, P. M.; Ortí, E.; Torres, T.; González-Rodríguez, D. Non-Centrosymmetric Homochiral Supramolecular Polymers of Tetrahedral Subphthalocyanine Molecules. *Angew. Chem. Int. Ed.* **2015**, *54*, 2543–2547.

(31) Gorbunov, A. V.; Iglesias, M. G.; Guilleme, J.; Cornelissen, T. D.; Roelofs, W. S. C.; Torres, T.; González-Rodríguez, D.; Meijer, E. W.; Kemerink, M. Ferroelectric self-assembled molecular materials showing both rectifying and switchable conductivity. *Sci. Adv.* **2017**, *3*, e1701017.

(32) Adachi, K.; Watarai, H. Site-Selective Formation of Optically Active Inclusion Complexes of Alkoxo-Subphthalocyanines with Β - Cyclodextrin at the Toluene/Water Interface. *Chem. –Eur. J.* **2006**, *12*, 4249–4260.

(33) Xu, H.; Ermilov, E. A.; Röder, B.; Ng, D. K. Formation and Energy Transfer Property of a Subphthalocyanine-Porphyrin Complex Held by Host-Guest Interactions. *Phys. Chem. Chem. Phys.* **2010**, *12*, 7366–7370.

(34) Guilleme, J.; González-Rodríguez, D.; Torres, T. Triflate-Subphthalocyanines: Versatile, Reactive Intermediates for Axial Functionalization at the Boron Atom. *Angew. Chem. Int. Ed.* **2011**, *50*, 3506–3509.

(35) PonceL, P; Fomina, L; Perez, F; Fomine, S. Unusual behaviour of bis[ω-hydroxyalkyl]-1,8,4,5-naphthalenetetracarboxylic bisimides in bisimide–lactam ring contraction: experimental and theoretical study. *J. Mol. Struct.* **2001**, *541*, 131–139.

(36) de Rouville, H.-P.; Iehl, J.; Bruns, C. J.; McGrier, P. L.; Frasconi, M.; Sarjeant, A. A.; Stoddart, F. J. A Neutral Naphthalene Diimide [2]Rotaxane. *Org. Lett.* **2012**, *14*, 5188–5191.

(37) Paton, A. S.; Morse, G. E.; Lough, A. J.; Bender, T. P. Observations Regarding the Crystal Structures of Non-Halogenated Phenoxyboronsubphthalocyanines Having Para Substituents on the Phenoxy Group. *CrystEngComm* **2010**, *13*, 914–919.

(38) (a) Asakawa, M.; Ashton, P. R.; Ballardini, R.; Balzani, V.; Bělohradský, M.; Gandolfi, M.; Kocian, O.; Prodi, L.; Raymo, F. M.; Stoddart, F. J.; Venturi, M. The Slipping Approach to Self-Assembling [n]Rotaxanes. *J. Am. Chem. Soc.* **1997**, *119*, 302–310. (b) Ashton, P. R.; Bělohradský, M.; Philp, D.; Stoddart, J. F. Slippage—an Alternative Method for Assembling [2]Rotaxanes. *J. Chem. Soc. Chem. Commun.* **1993**, 1269–1274. (c) Ashton, P. R.; Baxter, I.; Fyfe, M. C. T.; Ryamo, F. M.; Spencer, N.; Stoddart, J. F.; White, A. J. P.; Williams, D. J. Rotaxane or Pseudorotaxane? That Is the Question! *J. Am. Chem. Soc.* **1998**, *120*, 2297–2307. (d) Catalán, A. C.; Tiburcio, J. Self-Assembly of Pseudo-Rotaxane and Rotaxane Complexes Using an Electrostatic Slippage Approach. *Chem. Commun.* **2016**, *52*, 9526–9529.

(39) Cubberley, M. S.; Iverson, B. L. ^{1}H NMR Investigation of Solvent Effects in Aromatic Stacking Interactions. *J. Am. Soc. Chem.* **2001**, *123*, 7560–7563.

(40) Prentice, G. M.; Pascu, S. I.; Filip, S. V.; West, K. R.; Pantoș, G. D. Aromatic Donor-Acceptor Interactions in Non-Polar Environments. *Chem. Commun.* **2015**, *51*, 8265–8268.

(41) El-Khouly, M. E.; Kim, J.-H.; Kim, J.-H.; Kay, K.-Y.; Fukuzumi, S. Subphthalocyanines as Light-Harvesting Electron Donor and Electron Acceptor in Artificial Photosynthetic Systems. *J. Phys. Chem. C* **2012**, *116*, 19709–19717.